Modelling the Material Properties and Behaviour of Multicomponent Alloys

N. Saunders[1], Z. Guo[2], A.P. Miodownik[1] and J.-Ph.Schillé[2]

[1]Thermotech Ltd., Surrey Technology Centre, The Surrey Research Park
Guildford GU2 7YG, U.K.

[2]Sente Software Ltd., Surrey Technology Centre, The Surrey Research Park
Guildford GU2 7YG, U.K.

Summary

This paper describes the development of a new multi-platform software programme called JMatPro for calculating the properties and behaviour of multi-component alloys. These properties are wide ranging, including

- Thermo-physical and physical properties (from room temperature to the liquid state)
- Temperature and strain dependent mechanical properties up to the liquid state.
- TTT/CCT diagrams of steels, Al-alloys, Ni-based superalloys, Ti-alloys.
- Physical and mechanical properties of steels as a function of time/temperature/cooling rate during cooling.

A feature of the new programme is that the calculations are based on sound physical principles rather than purely statistical methods. Thus many of the shortcomings of methods such as regression analysis can be overcome. It allows sensitivity to microstructure to be included for many of the properties and also means that the true inter-relationship between properties can be developed, for example in the modelling of creep and precipitation hardening. This paper will show numerous examples of calculated results for various properties in Al-, Fe- and Ni-based alloys with the emphasis being placed on validation of calculated results against experimental observation in multi-component commercial alloys.

Keywords

Material properties, high temperature strength, solidification, TTT diagrams, quench distortion

1. Introduction

The physical, thermo-physical and mechanical properties of materials are a vital input for process modelling. However, while such properties are relatively easy to measure at room temperature, they become increasingly difficult to determine experimentally at high temperatures. Also, with regard to flow, properties become increasingly difficult to measure at high strain strates and in steep temperature gradients. To overcome these difficulties and to provide reliable and cost effective data for process modelling, sound models are required so that such properties can be readily calculated. The present paper provides background to a new software package JMatPro [1,2,3,4,5] that is able to provide many of the properties required.

A feature of the new programme is that the models are based on sound physical principles rather than purely statistical methods. Thus many of the shortcomings of methods such as regression analysis can be overcome. It allows sensitivity to microstructure to be included for many of the properties and also means that a true inter-relationship between properties can be developed. This presentation will show numerous examples of calculated results for various properties in multi-component alloys, concentrating on three areas.

- Use in solidification modelling.
- High temperature mechanical properties.
- Phase transformations in steels leading to quench distortion.

2. Use in Solidification Modelling

The physical and thermo-physical properties of the liquid and solid phases are critical information for the casting industry. Such properties include the fraction solid transformed, heat release, thermal conductivity, volume, density and viscosity, all as a function of temperature. Due to the difficulty in experimentally determining such properties during casting/solidification process, little information exists for multi-component alloys. Within the framework of the development of JMatPro, extensive work has been carried out on the development of sound, physically based models for these properties [3,4,5]. As well as providing comprehensive data for all critical properties, it is possible to examine (a) how changes in the composition of an alloy within its specification range can substantially affect properties during solidification, and (b) how properties of the liquid can substantially vary in the mushy zone, rendering simple extrapolation of high temperature experimental data inadequate for estimating properties in the mushy zone.

The first example we will examine is the Al-alloy ADC12 (Japanese designation). This is a high Si and Cu alloy with quite large variations of the admissible levels of elements such as Cu, Fe, Ni and Si. Two compositions have been tested; one at the minimum level specified for each element, the other

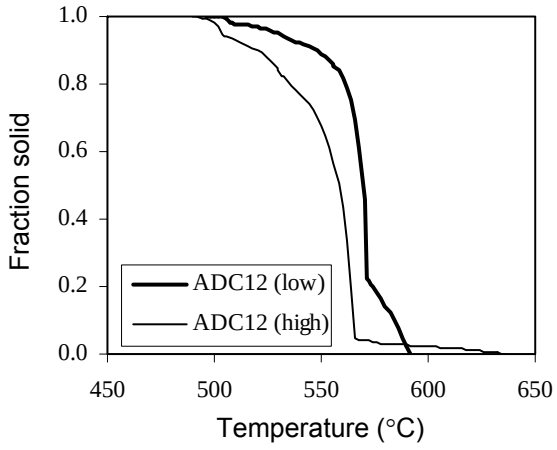

Figure 1. Calculated fraction solid vs. temperature plots of two ADC12 Al-alloys.

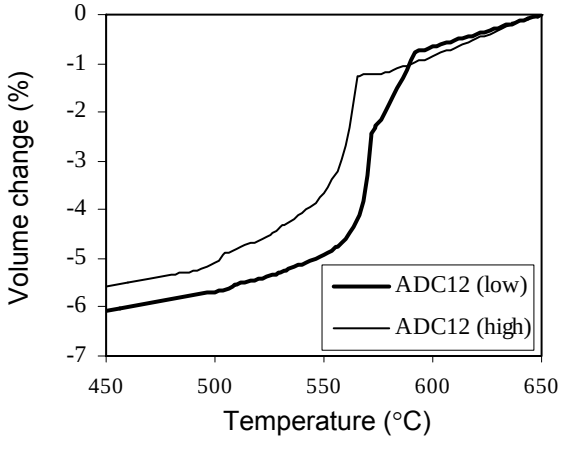

Figure 2. Calculated volume change vs. temperature plots of two ADC12 Al-alloys.

the maximum level. While such a choice might be expected to show the largest difference in behaviour, this is not necessarily the case. Depending on the partition coefficient and effect on invariant reactions, it is possible for an increase in one element to cancel out the effect of another. In the event, the calculated difference in behaviour of the two ADC12 alloys is very striking.

Figure 1 shows the fraction solid vs. temperature plots for the two alloys. The high specification (HS) alloy is hypereutectic, with primary Si and intermetallics forming over a significant temperature range, while the low specification (LS) alloy forms about 22% primary Al. At the start temperature of eutectic solidification for the HS alloy (565ºC) the fraction solid for the LS alloy is ~65%, in comparison to ~5% for the HS alloy. The discrepancies between fraction solid at any temperature remain high for much of solidification sequence, though both finally solidify via a eutectic involving Al_2Cu. Due to the very different behaviour of the two alloys, there will be a subsequent effect on all of the properties as a function of temperature. An example is the volume change in the range 450-650ºC, which again is quite different for the two alloys (Figure 2).

Differences between alloys with much smaller composition variations can produce quite substantial variations in the behaviour of the physical properties of the liquid. The Al-alloy 356 is taken as an example in the present paper. Figure 3 shows the density changes of an alloy with the composition Al-0.01Cu-0.2Fe-0.3Mg-0.02Mn-7Si-0.025Zn (wt%). For this composition, there is a slight density inversion as Mg segregates into the liquid below the Silicon eutectic. However, when Cu, Mn and Zn levels increase to higher levels (0.25%Cu, 0.3Mn, 0.35Zn) the behaviour of the liquid in the mushy zone changes dramatically (Figure 4). The initial dendritic Al solidification is very similar; however the behaviour during the eutectic part of solidification is quite different, with the liquid phase now being much denser. The viscosity is also much changed and both effects will strongly affect liquid flow in the dendrite arms and hence defect formation.

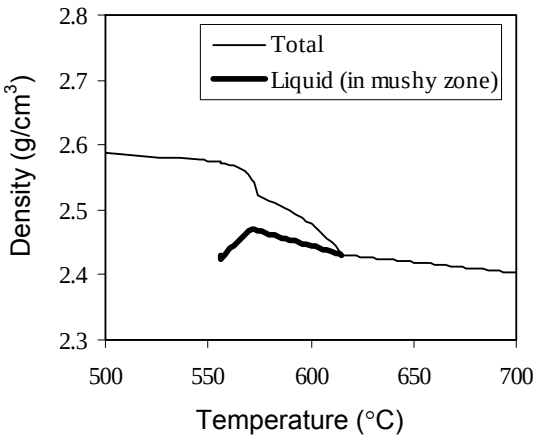

Figure 3. Calculated density of a 356 Al-alloy (with low Cu, Mn and Zn) during solidification. The bold line shows density of the liquid in the mushy zone

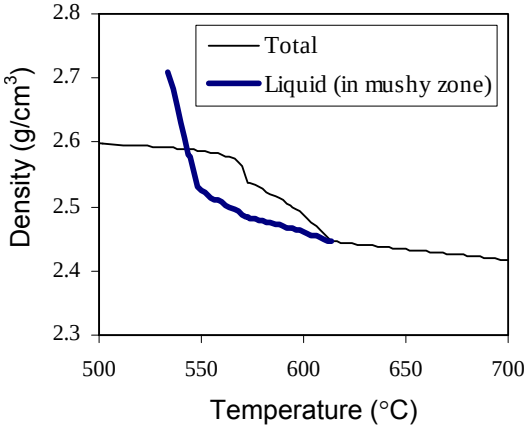

Figure 4. Calculated density of a 356 Al-alloy (with high Cu, Mn and Zn) during solidification. The bold line shows density of the liquid in the mushy zone

3. High Temperature Mechanical Properties

A key element in process modelling of metallic alloy is their high temperature mechanical behaviour, particularly with respect to flow stress as a function of temperature and strain rate. Many attempts at modelling flow behaviour in metals utilise constitutive equations, which are fitted to experimental results. This allows some extrapolation from the regime of temperature and strain rate of the experiment, but confidence in the result when well away from the experimental regime declines considerably. It is therefore of substantial interest to develop physically based models that can be self-consistently applied and which can both account for known experimental data and be extrapolated into new and very different regimes with greater confidence.

The modelling method in JMatPro utilises well-established strength equations for low temperature dislocation yielding and utilises the classic Hall-Petch equation to provide strength as a function of grain size [1,2, 5]. The model utilises a generalised pair interaction approach for solid solution strengthening that has been validated for many types of alloys, including steels, Ti-alloys and Ni-based alloys. Models of precipitation hardening have also been developed and tested for Ni-based alloys [1,2,5] and will be extended to more general cases, such as carbide hardening.

Generally speaking, room temperature strength decays monotonically with increasing temperature until the point where it enters into a temperature regime whereby there is a sharp fall in strength and flow stress becomes much more strongly dependent on strain rate. This region coincides exactly with the stress/temperature range where flow is governed by creep [1,2,5].

Several algebraic relationships between visco-plastic flow and creep are available in the literature [6,7], but the perceived difficulty in obtaining the necessary input parameters to creep equations has meant that this area of research has not been well developed. JMatPro has developed creep models based on classic creep formulations that have been extensively validated against experiment for steels and Ni-based superalloys. Such equations both accurately predict known high temperature flow stress and, because the input parameters are physically based (e.g. diffusion mechanisms, fault energies), they provide a much greater ability to be used outside of previously measured stress/strain rate/temperature regimes.

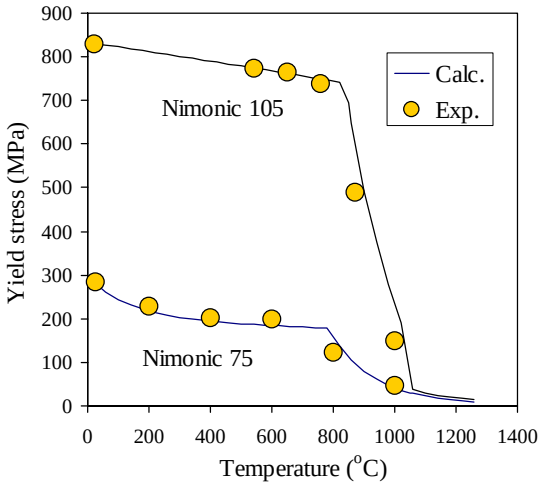

Figure 5. Comparison between experimental and calculated yield stress for Nimonic 75 and 105 as a function of temperature.

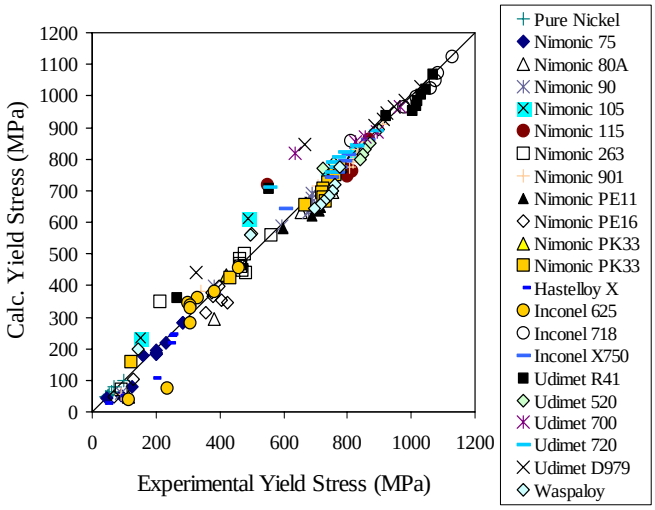

Figure 6. Comparison between experimental and calculated yield stresst for various wrought superalloys and pure Ni between RT and 1000ºC.

Fig. 5 shows the yield stress of two Ni-based superalloys, one precipitation hardened by gamma' (Nimonic 105) the other a solid solution alloy (Nimonic 75). The model correctly predicts the transition where sudden softening occurs and can also account for the loss of strength as the gamma' dissolves and the alloy eventually becomes a solid solution. To emphasise the predictive capability of the model, Figure 6 shows the calculated yield stress of 22 commercial superalloys as a function temperature between room temperature (RT) and 1000ºC. The 22 alloys comprise a wide variety of alloy types, ranging from pure Ni, to high alloyed solid solution types such as the Hastelloy series to high γ' type alloys such as the Udimet series that can contain up to 50%γ'. Figure 7 shows a similar plot for a variety of stainless steels, including austenitic, ferritic and duplex types.

Flow stress as a function of strain rate has also been calculated and Figure 8 shows such a series of calculated yield stress for a 316 stainless steel at as the strain rate is increased from 0.0001 s^{-1} to 1 s^{-1}. The transition from a dislocation yield mechanism to a creep controlled mechanism is clearly observed and is substantially displaced. However, even at a rate of 1 s^{-1}, creep is still the dominant mechanism above 1000ºC.

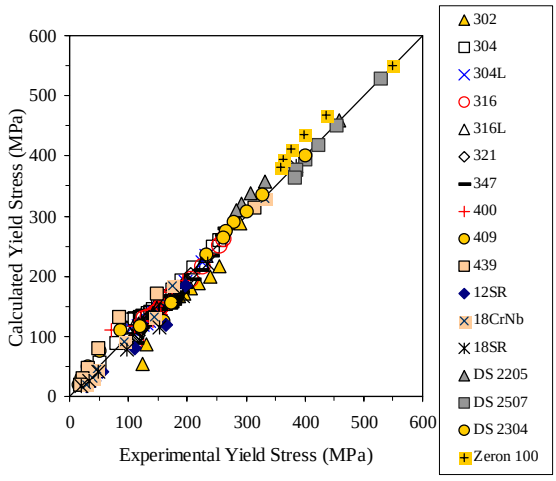

Figure 7. Comparison between experimental and calculated yield stress for various stainless steels between RT and 900ºC.

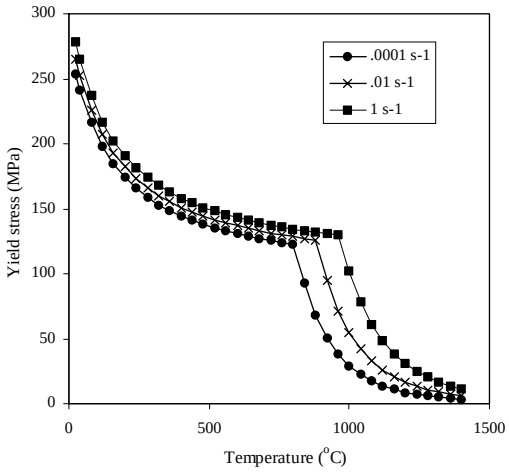

Figure 8. Calculated yield stresses for a 316 stainless steel as a function of strain rate and temperature.

Of particular interest is to note that the strain rate dependency at any temperature in the creep controlled regime is substantially greater than in the dislocation yield controlled regime. For example at 1100ºC, the yield stress increases by almost a factor 4 between 0.0001 and 1 s^{-1}.

4. Phase Transformations in Steels Leading to Quench Distortion

Knowledge of the Time-Temperature-Transformation (TTT) or Continuous-Cooling-Transformation (CCT) diagrams of steels is an important factor in the thermo-mechanical processing of steels. Much experimental work has been undertaken to determine such diagrams. However, the combination of wide alloy specification ranges, coupled with sharp sensitivity to composition changes plus a dependency on grain size, means that it is impossible to experimentally produce enough diagrams for generalised use. To this end significant work has been undertaken over recent decades to develop models that can calculate TTT and CCT diagrams for steels. Almost without exception, these models have been shown to be limited in applicability to carbon and low alloy steels.

The aim of the present work is to develop a model that can provide accurate TTT and CCT diagrams for a much wider range of steels, including medium to high alloy types, tool steels, 13%Cr steels etc.. By linking such calculations to JMatPro's property models a complete set of physical and mechanical properties can be calculated for steels as a function time/temperature/cooling rate. Additionally such calculations must be able to account for complex cooling paths that result from modern heat treatments.

The main aim of such work has been realised and JMatPro is now able to calculate TTT and CCT diagrams for steels of all types. This has been achieved by using Kirkaldy's model as a starting point [8, but modifying it extensively so that it can be applied to high alloy types. Figure 9 shows TTT diagrams calculated for four very different types of steels (a) a low alloy 4140 steel, (b) a high carbon, medium alloyed NiCrMo steel, (c) a T1 high speed tool steel and (d) a 13% Cr steel including comparison with experiment for all cases

While Figure 9 provides detailed results for specific alloys, it is instructive to look at overall accuracy of the calculations. To this end we have taken the experimentally observed times at the nose temperature of the C-curves denoting the start of transformation to ferrite, pearlite and bainite and compared these to those calculated using the new model. In this way it is possible to gain a good measure of the overall accuracy. In some cases, particularly for fast transformation steels, it was not possible to clearly differentiate the nose temperatures for the various transformations. For example, the ferrite, bainite and pearlite transformations appear merged into a continuous C-curve in the experimental work. In such circumstances, the calculated transformation of the fastest phase was taken.

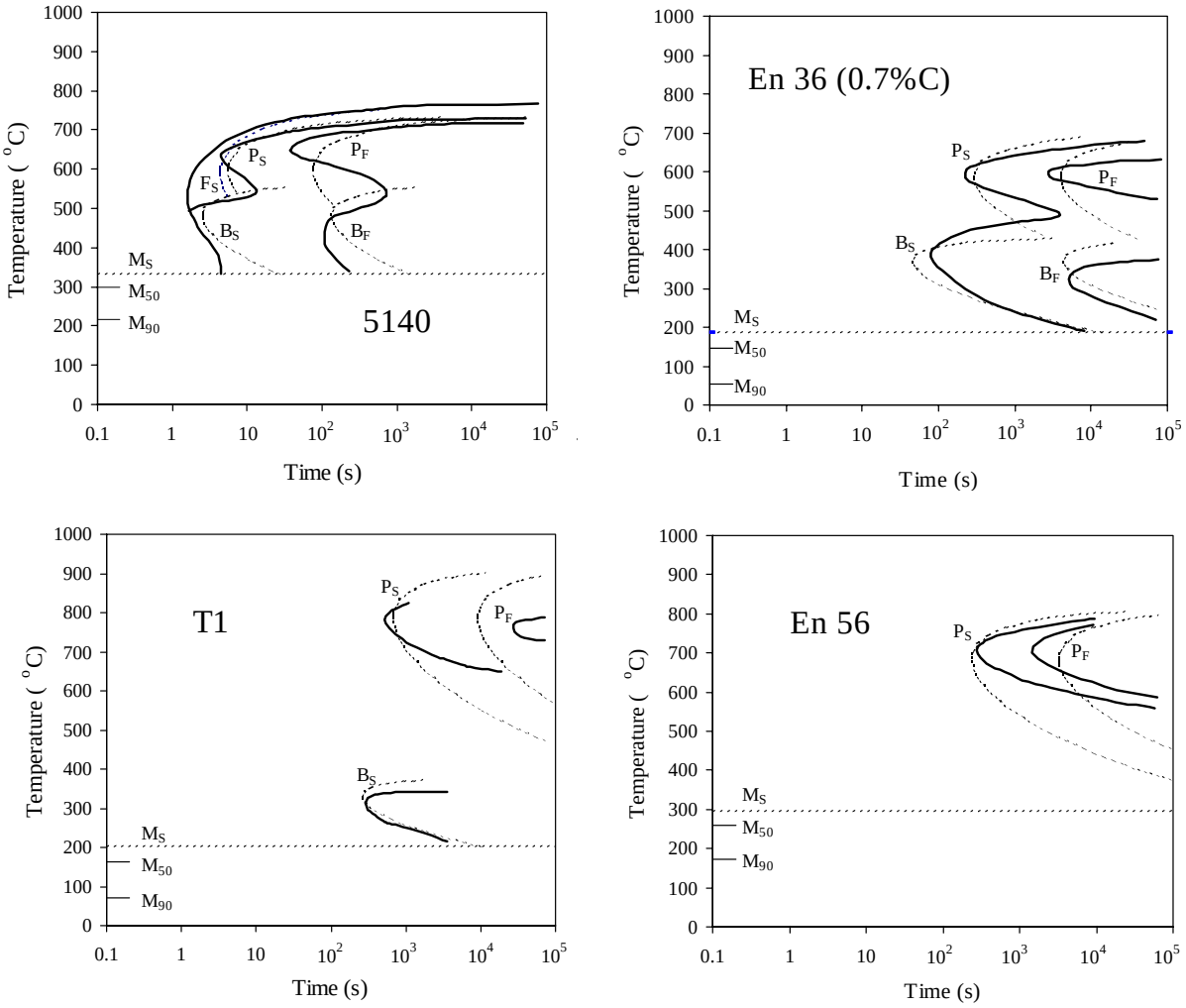

Figure 9. Comparison between experimental and calculated TTT diagrams for various steels

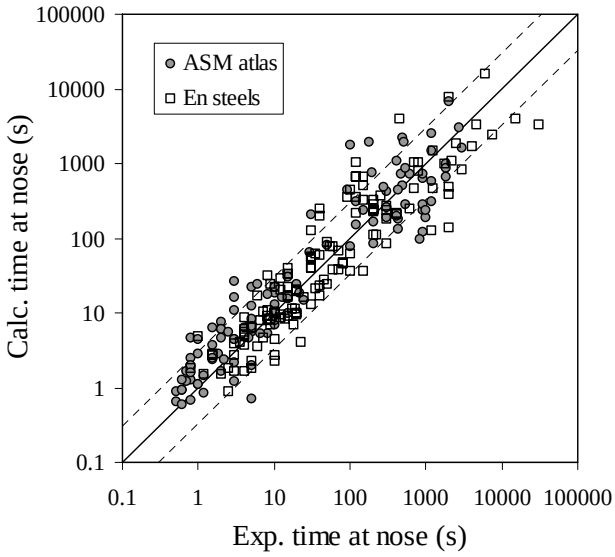

Figure 10. Comparison between experimental and calculated times at the nose temperature of the start C-curves for various steels.

The results have been broken down for comparison (Figure 10) between British En steels [9] and ASM atlas steels [10]. We have avoided "double counting" where the same steels are shown both in the En steel atlas and the ASM atlas. In particular, the En steel atlas has extensive coverage for NiCr and NiCrMo steels and, as such, comparison is made only to the En steel atlas for such alloys. In Figure 10 the dashed lines representing an error of 3x and have been included for guidance.

The comparison between calculation and experiment is very good and represents a substantial advance over previous models whose range of validity is largely confined to C and low alloy steels. It is further instructive to analyse the results in terms of statistical accuracy, which shows that 80% of calculated results are within a factor of 3 of experiment while almost 90% lie within a factor of 4. To emphasise the high levels of alloying that

have been used in the comparison studies, Table 1 shows the maximum levels of particular elements added as well as the lowest level of Fe in any one alloy.

Table 1. Maximum level of alloying addition in steels used for validation of model. Also shown is the minimum level of Fe.

	max/min level		max level		max level
Fe	> 75	Ni	< 8.9	W	< 18.6
C	< 2.3	Cr	< 13.3	Al	< 1.3
Si	< 3.8	Mo	< 4.7	Cu	< 1.5
Mn	< 1.9	V	< 2.1	Co	< 5.0

It is quite simple to transform the model such that it calculates phase formation as a function of time and temperature during a cooling cycle. The cooling path can be quite arbitrary, including isothermal hold times at constant temperature, if required. For demonstration purposes we have chosen a 4140 US grade steel and calculated various properties on heating and at cooling rates ranging from 0.01 to 100 K s^{-1} (Figure 11).

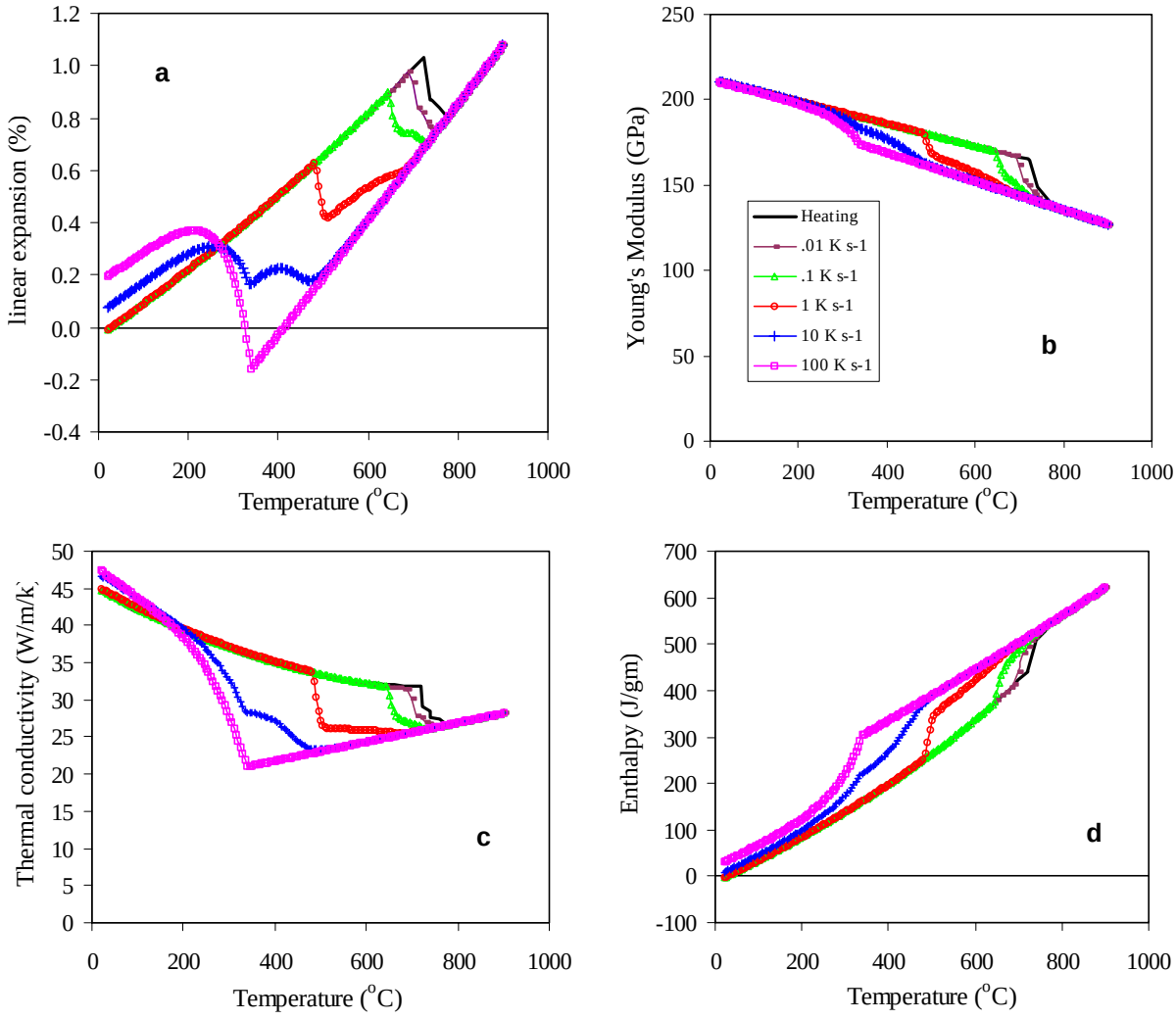

Figure 11. Various properties calculated for a 4140 steel (US Designation) on heating and at cooling rates ranging from 0.01 to 100 K s^{-1}.

c d

5. Summary

The paper has shown how a new software programme, called JMatPro, has been able to calculate a variety of material properties and behaviour for multi-component alloys. In particular, the paper has concentrated on JMatPro's capability for

- Solidification modelling.
- High temperature mechanical properties.
- Phase transformations in steels leading to quench distortion.

The new programme emphasises calculation methods that are based on sound physical principles rather than purely statistical methods. In this way, many of the shortcomings of methods such as regression analysis are overcome. The inclusion of microstructurally sensitive parameters means that it is possible to make the link with materials models that are currently being developed for prediction of microstructure. This makes it quite feasible to foresee, in the near future, the development of a true virtual capability for design and optimisation of thermo-mechanical heat treatment schedules for many different types of new alloys as well as existing ones. A key factor in the success of the approach has been the extensive validation of calculated results against experiment.

References

[T1] N. Saunders, X. Li, A.P. Miodownik and J-Ph. Schillé, "Materials Design Approaches and Experiences", eds. J.-C. Zhao et al., TMS, Warrendale, PA, 2001, p. 185.

[2] N. Saunders, Z. Guo, X. Li, A.P. Miodownik and J-Ph. Schillé, JOM, 55(12), 2003, p. 60.

[3] N. Saunders, X. Li. A.P. Miodownik and J.-Ph. Schillé, "Modelling of Casting, Welding and Advanced Solidification Processes X", eds. D. Stefanescu et al., TMS, Warrendale, PA, 2003, p. 669.

[4] Z. Guo, N. Saunders, A.P. Miodownik, J.P. Schillé, "Modelling of Casting and Solidification Processes 2004", ed. H. Weng-Sing, Metal Industrials Research and Development Centre, Kaohsiung, Taiwan, 2004, p. 563.

[5] N. Saunders, Z. Guo, X. Li, A.P. Miodownik and J-Ph. Schillé, "Superalloys 2004", Eds. K.A. Green et al., TMS, Warrendale, PA, 2004, p. 849.

[6] K. Harste and K. Schwedtfeger, Mater. Sci. Tech., 8, 1992, p. 23.

[7] K. Harste and K. Schwedtfeger, Mater. Sci. Tech., 12, 1996, p. 378.

[8] J.S. Kirkaldy and D.Venugopolan, "Phase Transformations in Ferrous Alloys", eds. A.R. Marder and J.I. Goldstein, AIME, Warrendale, PA, 1984, p. 125.

[9] "Atlas of Isothermal Transformation Diagrams of BS En Steels", Special report No.56 (London: The Iron and Steel Institute, 1956)

[10] "Atlas of Isothermal Transformation and Cooling Transformation Diagrams", (Metals Park, OH: 1977).